

# Orientation of Dye Molecules in DNA-Based Films with Chain Alignment and Judgment of Their DNA-Binding Modes

Nahoko Morii,<sup>\*,†,‡</sup> Giyuu Kido,<sup>\*,§</sup> Takeo Konakahara,<sup>||</sup> and Hisayuki Morii<sup>⊥</sup>

*Nanomaterials Laboratory, National Institute for Materials Science (NIMS), Tsukuba, Ibaraki 305-0003, Japan, Tsukuba Magnet Laboratory, National Institute for Materials Science (NIMS), Tsukuba, Ibaraki 305-0003, Japan, Department of Pure and Applied Chemistry, Faculty of Science and Technology, Tokyo University of Science (RIKADAI), Noda, Chiba 278-8510, Japan, and Protein Dynamics Research Group, National Institute of Advanced Industrial Science and Technology (AIST), Tsukuba, Ibaraki 305-8566, Japan*

*Received: April 10, 2005; In Final Form: June 20, 2005*

Novel composite films of chain-oriented DNA, which contain the DNA-binding dyes aligned in specific orientation, were successfully prepared by drying the solution under a horizontal magnetic field. Most of the dye–DNA composite films showed linear dichroism, as revealed by polarized ultraviolet–visible (UV–vis) spectroscopy. The intercalators, ethidium bromide and acridine orange, were fixed in chain-oriented DNA films in a similar binding manner as in solutions. Also, Hoechst 33258 and 4',6-diamidino-2-phenylindole were found to be aligned along the minor groove, even in the solid films. Thus, our new method of preparing dye–DNA composite films with chain orientation is useful for aligning small molecules, and it will provide views of the novel anisotropic materials expected in various application fields. We used this method to prepare composite DNA films with newly designed original compounds. Seven of nine dyes were judged to bind obviously to DNA as intercalators by polarized UV–vis spectroscopy. The DNA-binding manners were further analyzed by fluorescence anisotropy measurements. On the basis of the curves for the rotational angle dependence of the anisotropy, we were able to estimate the angles between the transition-dipole moments of dyes and the aligned chain axis of DNA. Interestingly, two original compounds were found to be in the tilted forms with regard to the plane of base pairs. We emphasize here that the method using aligned dye–DNA films is very convenient for identifying the binding modes of the compounds for double-stranded DNA.

## Introduction

DNA is a unique material that has a specially constructed molecular architecture different from that of other general synthetic polymers. The double-stranded structure of DNA has an approximately 100-nm statistical chain element length, which is remarkably long in comparison with the 2-nm diameter. Therefore, DNA with adequate length is so rigid that it is recognized as a liquid crystalline polymer.<sup>1</sup> In a previous work, we reported that DNA films with well-oriented molecular chains can be obtained by both the magnetic effect and the concurrent interface-induced effect.<sup>2,3</sup> The behavior of DNA chains in a magnetic field is based on the anisotropic magnetic susceptibility of the base pairs.<sup>4,5</sup> However, if the interfacial effect to align the DNA chains does not work, the magnetic effect alone is not enough to induce the uniform orientation of DNA molecular chains. Therefore, it is important to dissolve the natural DNA materials in water at a lower concentration than that showing the liquid crystalline property.<sup>6,7</sup> This method for molecular chain alignment can be expected to have a different

range of application from the melt-drawing method to fabricate typical polymeric materials.

DNA has been highlighted as a distinctively characteristic polymer in recent years, and fundamental research on the use of DNA in electronic and optical devices has been occurring.<sup>8,9</sup> The synthetic DNAs with non-natural base pairs are notable examples of such functional materials.<sup>10,11</sup> For this purpose, the anisotropy of the materials is one of the important properties that may enhance their functionality. Several methods have been proposed to realize the anisotropy, including the Langmuir–Blodgett method using a monolayer of cationic lipid with DNA and the mechanical stretching method for DNA–lipid conjugates.<sup>12,13</sup> Also, the stretched films of poly(vinyl alcohol) are known to be an excellent host for orienting DNA as well as general dye molecules.<sup>14</sup> Our method of using anisotropic DNA film with oriented molecular chains is unique because the matrix of the material is made of only DNA. In this paper, we report that novel DNA-based materials with oriented dyes can be successfully fabricated.

The binding type of a dye to DNA has been estimated mostly by sedimentation, flow dichroism, fluorescence-detected flow dichroism, viscosimetry, and crystallography with synthetic DNA.<sup>15–17</sup> The clarification of the binding mode of novel pharmaceuticals such as synthetic antibiotics is so important that a method with simplicity, readiness, and reproducibility is expected in the course of development. In the present work, we applied our magnetic method for orientation of DNA molecular chains to the judgment of binding mode. The dye samples were prepared by drying DNA solution containing even

\* To whom correspondence should be addressed. Phone: +81-29-863-5359. Fax: +81-29-863-5514. E-mail: morii.nahoko@nims.go.jp.

† Nanomaterials Laboratory, National Institute for Materials Science (NIMS).

‡ Project of Support and Cooperation for Prior Researches, committed by Japan Science and Technology Corporation.

§ Tsukuba Magnet Laboratory, National Institute for Materials Science (NIMS).

|| Tokyo University of Science (RIKADAI).

⊥ National Institute of Advanced Industrial Science and Technology (AIST).

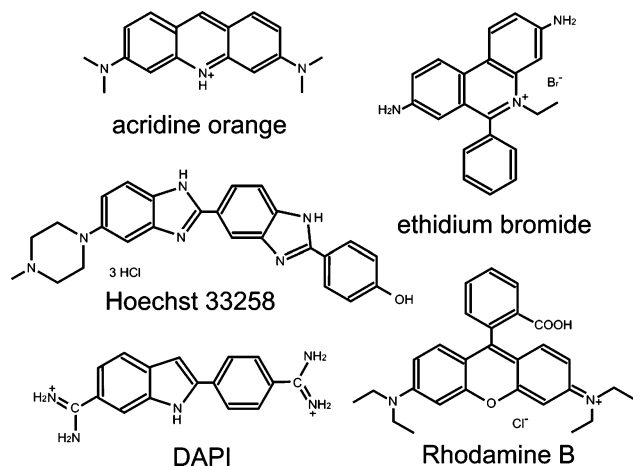


**Figure 1.** Molecular structures of the dyes. These are abbreviated in the text as AcrO, EtdB, Hoech, DAPI, and RhoB.

0.1  $\mu\text{g}$  of dye under a magnetic field. It takes only a few minutes to dry the solution on the silica plate. A magnetic field was generated with a cryogen-free superconducting magnet bearing a wide bore diameter (over 10 cm) and high magnetic intensity (about 10 T). The wide bore enables simultaneous processing for dozens of samples. The obtained dye–DNA films are stable for several months. The binding mode of a dye can be easily judged by ultraviolet–visible (UV–vis) spectroscopy and more precisely by fluorescence spectroscopy with polarization plates.

## Materials and Methods

**Chemicals.** Commercial DNA material derived from salmon sperm was used throughout the study. Fibrous DNA sodium salt purchased from BioChem (Japan) was dissolved in water followed by still-standing in a refrigerator for a month. Then, the supernatant was used for film formation. The initial concentration of DNA was adjusted to 90 mM<sub>bp</sub> (concentration for base pairs) at pH 6.8 without any additional buffer component. The dyes used were ethidium bromide (EtdB), acridine orange (AcrO), Hoechst 33258 (Hoech), 4',6-diamidino-2-phenylindole dihydrochloride (DAPI), and rhodamine B (RhoB). The formulas of these dyes are shown in Figure 1. EtdB, AcrO, DAPI, and RhoB were purchased from Wako Pure Chemicals (Japan). Hoech was purchased from Molecular Probes (U.S.A.). Commercial poly(acrylic acid) with an averaged molecular weight (MW) of 250 000 was dissolved and adjusted to pH 7 by the addition of aqueous NaOH. We used poly(vinyl alcohol) with a mean degree of polymerization of about 3500, which is a partially hydrolyzed material with a saponification value of 86–90 mol %. Poly(vinyl pyrrolidone) K90 with a MW of 360 000 was used after dissolving it in water. These polymers were purchased from Wako Pure Chemicals (Japan).

The novel DNA-binding reagents (Figure 8), which were originally designed and synthesized by one of the authors (T.K.), were used to prepare the dye–DNA films. Dimethyl sulfoxide used for the preservation in some of these dyes was removed by reversed-phase HPLC with a gradient elution of acetonitrile 15–45% before use.

**Preparation of Dye–DNA and Dye–Polymer Films.** The dyes were dissolved in water and mixed with DNA solution, of which the concentrations were adjusted to be 2 mM and 50 mM<sub>bp</sub>, respectively, unless otherwise indicated. An aliquot (3  $\mu\text{L}$ ) of dye–DNA solution was put in an 8-mm diameter circular region on a 25  $\times$  25  $\times$  1 mm silica plate, which had been

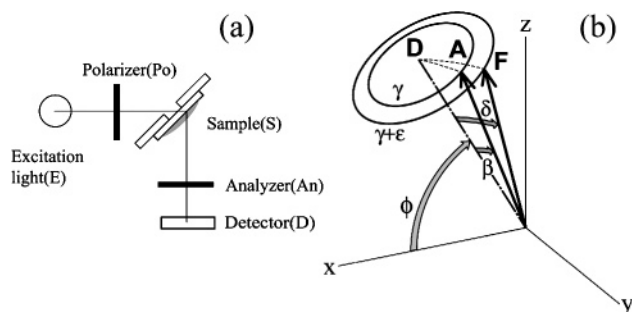


**Figure 2.** Optical system for the fluorescence measurements (a) and transition-dipole moments (b). (a) The measurements for the anisotropy were carried out with a couple of near-ultraviolet–visible polarization plates (Po and An). The sample film on a silica plate was located at a position of 45° with respect to both the excitation light and the detector. A rotary sample stage was manually rotated every 30° steps. (b) The ideally oriented dye molecule was defined in the three-dimensional coordinate system. The dye–DNA film was placed on the  $x$ – $z$  plane and was rotated around the  $y$ -axis by the angle  $\phi$ . Both transition-dipole moments corresponding to absorption (A) and fluorescence emission (F) were assumed to orientate to the directions different from the axis of DNA molecular chain (D) by the angles  $\beta$  and  $\delta$ , respectively. These moment vectors were set equally distributed around the DNA axis to show rotational symmetry. The angle  $\gamma$  was introduced as an integral variable.

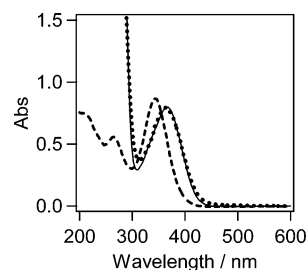


**Figure 3.** UV–vis spectra of Hoech-containing samples. The spectra of 0.02 mM Hoech solution in the presence and the absence of 0.50 mM<sub>bp</sub> DNA are indicated with a solid and a dashed curve, respectively. The spectrum of dye–DNA composite film containing 4 mol % Hoech is shown with a dotted curve. The thickness of the film was 1.5  $\mu\text{m}$ .

cleaned with an oxidizing reagent in advance.<sup>3</sup> For the polarization microscopic observation, we used 10  $\mu\text{L}$  of the solution. Just after the solution was deployed, the sample was introduced into the central spot of a magnet and was kept there until a dry film was formed. The space in the magnet bore was at 25 °C and 40–50% humidity. The magnetic intensity is 10 T, which is enough to align the DNA chains. The thickness of the membrane obtained from 3  $\mu\text{L}$  of solution was 1  $\mu\text{m}$ , which was determined with a Sony U30A digital indicator. The concentration of DNA was evaluated on the basis of the dry weight of fibrous DNA materials. In some cases, the relative concentrations of the solutions were determined by measuring the absorbance at 260 nm with an extinction coefficient of 13 200. The value 660 was adopted as the molecular weight of a base pair. The concentrations of dyes were based on their dry weights. AcrO and DAPI were used as monohydrates, as determined by elemental analysis.

The solution of AcrO– or Hoech–vinyl polymer for film formation contained 20 mg/mL of each polymer and 1.3 mM dye. The pH of the solutions was almost neutral (6.8–7.0). The thickness of the dry film prepared under the magnetic field was 1–20  $\mu\text{m}$ .

**Magnetic Field.** The magnetic field was generated with a cryogen-free superconducting magnet, the JASTEC-10T 100 mm (Japan Superconductor Technology, Inc.). An almost

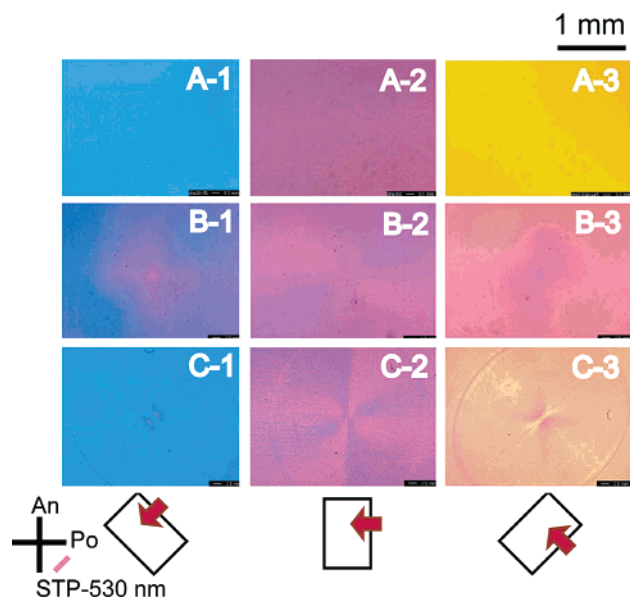


**Figure 4.** Polarization microscopic observation of dye–DNA films situated at three different angles. The picture was observed with a sensitive tint plate (STP), a polarizer filter (Po), and an analyzer filter (An). In the bottom illustration, the situation of the film is marked by a rectangle and the red arrows denote the direction of the magnetic field in the illustration. The pictures of DNA, EtdB–DNA, and Hoech–DNA films are shown in rows A, B, and C, respectively.

homogeneous magnetic field with accuracy within 1.5% was achieved in a spheric region with a diameter of at least 20 mm. The magnetic intensity was regulated to be 10 T. The magnet is cylindrical with a central bore 100 mm in diameter as a sample port. The horizontal magnetic field was applied to samples with the magnet lying in a horizontal position.

**Polarization Microscopy.** The dried DNA films were characterized with a polarization microscope (Olympus 60BX) equipped with crossed nicols. The samples were illuminated with a halogen lamp. To observe the mode of chain orientation, a coloring method with a 530-nm sensitive tint plate was adopted.

**Linear Dichroic UV–vis Spectroscopy.** The ultraviolet–visible (UV–vis) light absorption spectra were measured with a Shimadzu UV-1200 spectrophotometer. The optical system was set in the order of an illuminant, a polarizer, a sample, and a circular slit 5 mm in diameter. The incident light was polarized through a Glan–Taylor prism and was radiated from the surface of the film mounted on a silica plate. The optical polarization of dyes was evaluated by linear dichroism at the wavelength of maximum absorbance in the range from 350 to 650 nm. The spectral data were measured with and without a polarizer, which are designated here as  $I_V(\phi_{BP})$  and  $I_0(\phi_{BP})$ , respectively. The data were collected for the samples at the rotational angles increased by each 30° increment, using a rotary sample stage. The angle  $\phi_{BP}$  was defined as the angle between the magnetic vector marked at the time of film preparation and the direction of a polarizer.

To remove the influence of heterogeneity in the observed film area, we corrected the raw data to be the angular dependence of absorbance for polarization light,  $A_V(\phi_{BP})$ , using the following equation:

$$A_V(\phi_{BP}) = \frac{I_{av}}{I_0(\phi_{BP})} I_V(\phi_{BP}) \quad (1)$$

where  $I_{av}$  denotes the mean value of  $I_0(\phi_{BP})$  for  $\phi_{BP}$ . Essentially,

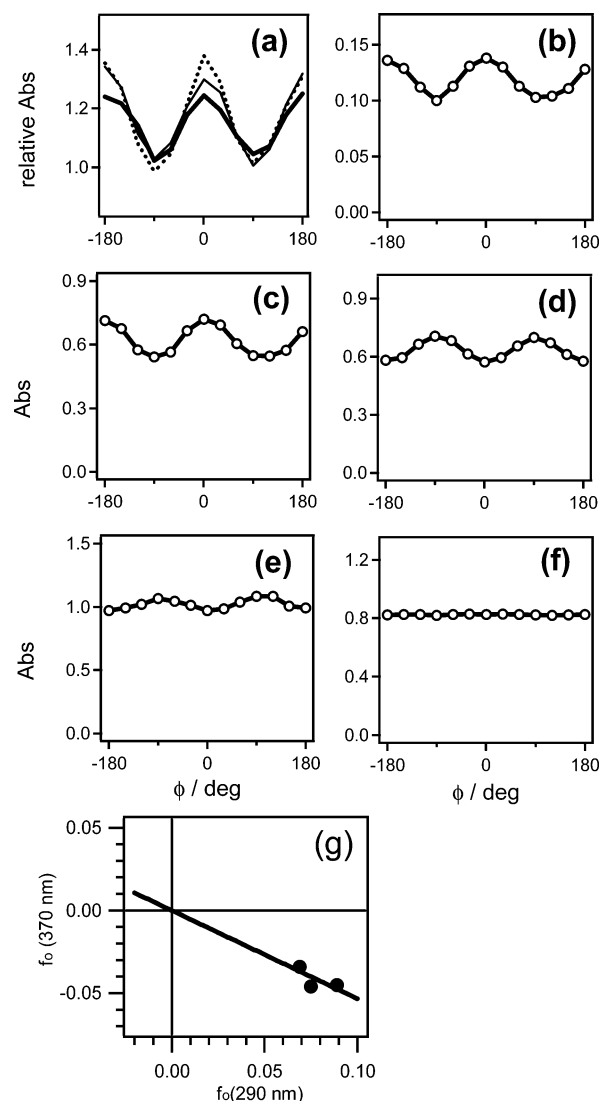


**Figure 5.** Angular dependence of the absorbance obtained by the linear polarization UV–vis measurement for the dye–DNA films. The abscissa shows the angle  $\phi$  between the magnetic vector marked at the time of film preparation and the direction of a polarizer. (a) The relative absorbances of DNA solid films prepared from the solutions at different concentrations—30, 60, and 90 mM<sub>bp</sub>—are shown with a thick solid, a thin solid, and a dotted line, respectively. The ordinate scale corresponds to the absorbance at 260 nm of the film from the solution of 90 mM<sub>bp</sub>. (b–f) Angular dependence curves were exhibited for dye–DNA films prepared at 4 mol % dye content with respect to DNA base pair. The dyes are EtdB (b), AcrO (c), Hoech (d), DAPI (e), and RhoB (f). (g) The values of  $f_0(290 \text{ nm})$  and  $f_0(370 \text{ nm})$  calculated from the angular dependence of the DAPI–DNA films were plotted. The parameters  $f_0(290 \text{ nm})$  and  $f_0(370 \text{ nm})$  represent the extents of the orientation for DNA base pair and for DAPI, respectively. The plotted values were obtained for the films prepared with the solutions containing 1, 3, and 6 mol % dye.

$A_V(\phi_{BP})$  changes according to the square sine function due to the interaction of an oriented transition-dipole moment and a polarization light, as described later (eq 6).

To evaluate the extent of polarization for the films, we fit the following approximate expression to the observed plots by the nonlinear least-squares method:

$$A^{\text{fit}}(\phi_{BP}) = a_1 \{1 + f_0(1 - 2 \sin^2 \phi_{BP})\} + a_2 \cos(\phi_{BP} - a_3) \quad (2)$$

The second term of this expression represents the undesired bias

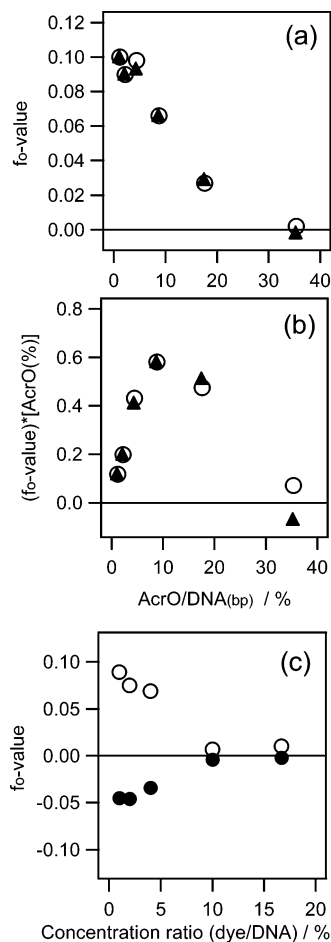


**Figure 6.** Dependence of  $f_0$  values on the dye contents. (a) The values of  $f_0(465\text{ nm})$  for AcrO dimer and  $f_0(514\text{ nm})$  for the monomer in AcrO–DNA films were plotted. The samples were prepared under the magnetic field from the solutions containing 1, 2, 4, 9, 18, and 35 mol % AcrO with respect to DNA base pairs. The closed triangles and the open circles represent  $f_0(465\text{ nm})$  and the  $f_0(514\text{ nm})$ , respectively. (b) The product of  $f_0$  value with the content of AcrO was shown for the same abscissa as that in Figure 6a. (c) The values of  $f_0(370\text{ nm})$  for DAPI and  $f_0(290\text{ nm})$  for DNA base pair in DAPI–DNA films were plotted. The films were prepared from the solutions containing 1, 2, 4, 10, and 17 mol % DAPI. The closed and open circles indicate  $f_0(370\text{ nm})$  and  $f_0(290\text{ nm})$ , respectively.

in a film, and the parameters  $a_1$ ,  $a_2$ , and  $a_3$  were used for the data fitting. For the uniaxially oriented samples, the measurements of only two absorption spectra with polarization parallel and/or perpendicular to the orientation axis are enough for the detection of linear dichroism. The result of this simple technique would be the same as that of the measurement for rotational angle dependence of absorbance. However, our method for the angular dependence is effective to eliminate the local nonuniformity of films, which affects the relative absorbance. The absolute value of the coefficient  $f_0$  indicates the fraction of a variable wave component with  $180^\circ$  periodicity.

**Fluorescence Anisotropy.** The fluorescence spectra were measured with a Shimadzu RF-5000 spectrofluorophotometer. The optical system was assembled with a pair of near-ultraviolet–visible polarization plates, HNPB (McCan Imaging Inc.), or the polarization filters for the visible region (Kenko Co., Ltd., Japan), as shown in Figure 2. The spectra were recorded through a vertical and/or horizontal polarizer for the sample at the angles rotated by each  $30^\circ$  interval. The sample film on a silica plate was located at a  $45^\circ$  angle with respect to both the illuminant and the detector. The angular dependence

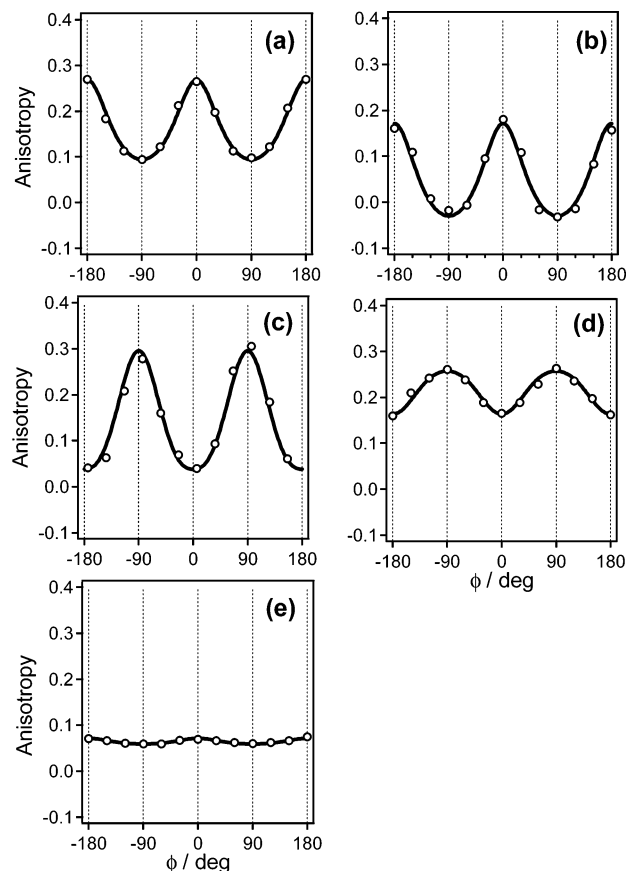


**Figure 7.** Angular dependence of the fluorescence anisotropy of the dye–DNA films. The observed and theoretical fluorescence anisotropy were exhibited with open circles and a solid curve. The abscissa  $\phi$  was defined as the angle between the magnetic vector given for the film and the direction of a polarizer. The dyes of DNA–composite films are EtdB (a), AcrO (b), Hoechst (c), DAPI (d), and RhoB (e). The data were collected for the  $3\text{-}\mu\text{m}$ -thick films with a dye content of 1 mol %.

of fluorescence anisotropy,  $R(\phi_{\text{BP}})$ , was calculated with the observed fluorescence intensities,  $F_{\text{VV}}(\phi_{\text{BP}})$  and  $F_{\text{VH}}(\phi_{\text{BP}})$ , as follows:

$$R(\phi_{\text{BP}}) = \frac{F_{\text{VV}}(\phi_{\text{BP}}) - G_{\lambda}F_{\text{VH}}(\phi_{\text{BP}})}{F_{\text{VV}}(\phi_{\text{BP}}) + 2G_{\lambda}F_{\text{VH}}(\phi_{\text{BP}})} \quad (3)$$

where  $G_{\lambda}$  is a correction factor for the intrinsic bias in the optical sensitivity of the detection system. Since the value of  $G_{\lambda}$  is dependent on the wavelength of the observation, it was estimated by the measurement with the solutions of the same dyes as those used for DNA–composite films. The factor  $G_{\lambda}$  was calculated as follows:

$$G_{\lambda} = \frac{F_{\text{HV}}}{F_{\text{HH}}} \quad (4)$$

To characterize the anisotropy of the films, the following approximate expression was fitted to the obtained plots by the least-squares method with the parameters  $a_4$  and  $a_5$ :

$$R^{\text{fit}}(\phi_{\text{BP}}) = a_4 R^{\text{theor}}(\phi_{\text{BP}}) + a_5 \quad (5)$$

The theoretical curve,  $R^{\text{theor}}(\phi_{\text{BP}})$ , was selected from the representative patterns calculated with eq 16, as described in the Supporting Information prior to the calculation of fitting.



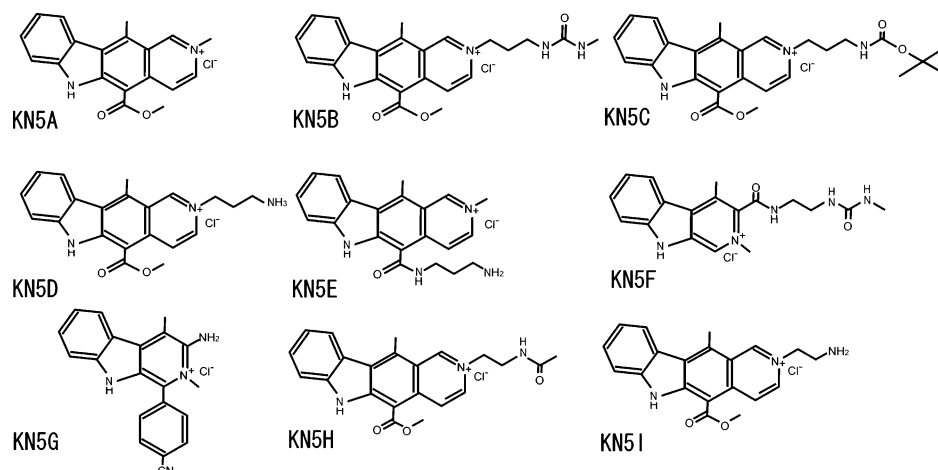


**Figure 8.** Molecular structures of the novel synthetic dyes developed for pharmaceutical purposes. The abbreviated compound names were shown beside the structural formulas.

**TABLE 1: Peak Wavelengths of the Specific Absorption for Commercial Dyes Observed by UV-vis Spectroscopy<sup>a</sup>**

sample	peak wavelength of dye/nm						
	(DNA)* <sup>1</sup>	Hoech	DAPI	EtdB	AcrO* <sup>2</sup>	AcrO* <sup>3</sup>	RhoB
dye soln		343	341	479	468	492	554
dye-DNA soln	260	366	358	524	476	502	554
dye-DNA film	260	364	360	526	477	502	565

<sup>a</sup> The concentrations of the dyes in the solutions were 0.02 mM. The DNA concentration in dye-DNA solution was 0.50 mM<sub>bp</sub>. The dye-DNA films contain 4 mol % dye with respect to the amount of DNA base pairs. (\*1, data without dyes; \*2 and \*3, wavelengths of a dimeric and a monomeric AcrO molecule, respectively.)

**Fundamental Equations for Optical Anisotropy.** To elucidate the anisotropy observed by UV-vis and fluorescence spectroscopy, we designed the theoretical equations on the basis of a model involving the ideally oriented dye molecules. The detailed equations are indicated in the Supporting Information. Here, only the equation of the absorbance,  $A_v$ , for the vertically polarized light is exhibited for convenience of the discussion as follows:

$$A_v = \frac{k_1}{2} \{ \sin^2 \beta + (3 \cos^2 \beta - 1) \sin^2 \phi \} \quad (6)$$

where the angle  $\beta$  indicates the tilt angle of the transition-dipole moments for absorption.

## Results and Discussion

**UV-vis Spectra of Dye-DNA Films.** The UV-vis spectra for five commercial dyes were observed in aqueous solution and DNA-containing solution and on DNA-composite film. The peak wavelengths of the specific absorption band are summarized in Table 1. The spectrum of Hoech in a solution shows the peak at 343 nm, whereas a red shift by  $\sim 20$  nm was observed in the presence of DNA, as shown in Figure 3. Its peak wavelength, 366 nm, was the same as that in dye-DNA film. It should be noted that the extents of red shift were almost common for dye-DNA solution and dye-DNA film in the cases of Hoech, DAPI, EtdB, and AcrO. In mixed solutions of DNA and dye, it is well-known that the interaction of electron orbits between DNA base pairs and dyes causes the red shift of absorption bands of dyes. On the basis of such characteristics, the intercalators are commonly used to detect and quantify the DNA. However, only RhoB behaved differently from the others, showing no shift in dye-DNA solution and a red shift in dye-

DNA film. This suggests that RhoB has special contact only in dye-DNA film. It seems possible that the substituent groups of the heterocycle in RhoB would destabilize the intercalating form between DNA base pairs. The measurement was carried out for the dye-DNA film with 1.5- $\mu$ m thickness, in which the concentration was significantly higher, by 6000 times, in contrast with the dye-DNA solution in a 10-mm cuvette. Nevertheless, the characteristics of the shape and peak wavelength were superimposed, so that the binding mode of dye and DNA in the solution seems to be inherited by the solid film.

**Polarization Microscopic Observation for Dye-DNA Films.** Figure 4 shows the polarization microscopic images of the dye-DNA films prepared under a magnetic field. The colors of dye-DNA films, which depend on the angle of the sample, were similar to those of the DNA film without dye. The small difference in apparent color of the dye-DNA film, as shown in Figure 4X-3 seems to be attributable to the color of dye itself. The observed color tone appears mainly to have reflected the birefringent of the DNA, because the dye contents in the dye-DNA films were very slight. The results mean that the DNA molecular chains aligned in a homogeneous direction by the magnetic effect irrespective of the presence or absence of the dyes. The direction of DNA chain alignment in any dye-DNA films was vertical with respect to the direction of the magnetic vector given for preparation.

**Linear Dichroism of Dye-DNA Films.** The linear polarization UV-vis spectra were measured at the point distant from the center by half the radius, where the color tone was especially homogeneous. Figure 5a shows the dependence of the absorbance at 260 nm on the rotational angle of molecular chain-oriented DNA films. The observed curves were well fitted with the square sine function, indicating the obvious linear dichroism derived from the aligned DNA chains perpendicular to the magnetic vector. Since the electronic transition-dipole moment at the 260-nm band arising from the  $\pi$ - $\pi^*$  transition of the DNA base pair is perpendicular to the chain axis, the signal intensity is weak when the molecular chains are parallel to a plane of polarization light. On the other hand, the signal intensity becomes strong when the chains are perpendicular to the polarization light plane. In this paper, we call the shape of such curves the "double-valley type" for convenience. To examine the effect of the initial DNA concentration, we prepared DNA solid films under a magnetic field from the solutions at concentrations of 30, 60, and 90 mM<sub>bp</sub>. Though the degree of polarization was somewhat large at a higher initial concentration of DNA, its change was not especially significant during the

course of the range of experiment, as shown in Figure 5a. Also, we found that the degree of polarization of DNA chains was not very much affected by the addition of dyes, of which the concentration was usually 2 mM in 50 mM<sub>bp</sub> DNA solutions.

The linear dichroism of the dye–DNA films prepared from five dyes under a magnetic field was also analyzed at the wavelengths of absorption bands for the dyes (Figure 5b–f). Except for RhoB, the other four dyes gave curves indicating linear dichroism, which suggests the specific orientation of these dyes in DNA films. The phase of curves for the linear dichroism of AcrO and EtdB was a double-valley type and consistent with that of DNA base pairs. This means that the electronic transition-dipole moments of these dyes orientate in a similar manner as that of the DNA base pairs. In contrast, Hoech and DAPI showed the curves for linear dichroism with a phase reversed against that of the DNA base pair. This reversal would be attributed to the electronic transition-dipole moment of dyes oriented along the DNA chain axes. The dye RhoB, which showed little difference in absorption wavelength between the dye solutions with and without DNA, had no apparent angular dependence for its absorbance (Figure 5f). This means that RhoB molecules are not oriented with respect to the DNA chains. Thus, there exists an explicit correlation between the spectral change caused by DNA in a solution and the linear dichroism of dye–DNA films. Most probably, both the location and the orientation of dye molecules, such as AcrO, EtdB, Hoech, and DAPI, in DNA solutions were fixed in DNA films by drying the solutions in a magnetic field. Therefore, the modes of dye orientation in DNA films would be the same as the binding types to DNA in solutions, which are the intercalation and the minor-groove binding.

**Comparison of the Degrees of Orientation.** The degree of orientation can be characterized with the parameter  $f_0$ , which is determined by fitting with eq 2 for an angular dependence curve of absorbance. Comparing the parameter  $f_0(260\text{ nm})$  for DNA base pairs and  $f_0(514\text{ nm})$  for the monomers of AcrO, the ratio  $f_0(514\text{ nm})/f_0(260\text{ nm})$  was found to be almost unity (1.07). This means that most of the AcrO monomers are bound with DNA base pairs as intercalators even in the DNA films.

In contrast, the dye–DNA film of DAPI known as a minor-groove-binding reagent at low dye contents exhibited a negative  $f_0(370\text{ nm})/f_0(290\text{ nm})$  value, which is the ratio of  $f_0$  at 370 nm for DAPI and that at 290 nm for DNA base pairs in the film. The ratio was estimated to be  $-0.56$  and was almost constant irrespective of the dye contents in the range below 3% (Figure 5g). That the absolute value of  $f_0(370\text{ nm})$  was about half that of  $f_0(290\text{ nm})$  seems to be ascribed to the tilt of the electronic transition-dipole moment with respect to the plane perpendicular to the DNA chain axis. If this tilt angle is constant, it can be calculated with the expression  $(3 \cos^2 \beta - 1)/(3 \cos^2(\pi/2) - 1) = f_0(370\text{ nm})/f_0(290\text{ nm})$ , which is derived from the second term of eq 6. In this case, the angle  $\beta$  resulted in  $44^\circ$ . This suggests that the longitudinal axis of DAPI was fixed along the DNA minor groove with a tilt angle of  $44^\circ$ . This value almost coincides with several reported ones, which are  $47^\circ$  determined by flow linear dichroism for a calf thymus DNA solution containing Hoech,  $45^\circ$  by X-ray crystallography for synthetic DNA with bound DAPI, and  $45^\circ$  by fluorescence energy transfer for DAPI–DNA solution.<sup>15,17,18</sup> Our result also indicates that most of the DAPI molecules bind to a minor groove in the oriented dye–DNA solid film. Though the binding types of DAPI are reported to be not only minor-groove binding but also the intercalation,<sup>18</sup> the tilt angle would not reflect the intercala-

tion of DAPI. This would be ascribed to the fact that the minor binding occurs predominantly at such low DAPI contents.

On the basis of our findings, we concluded that the orientation of both types of DNA-binding dyes reflects the DNA molecular chain orientation. To prove the importance of DNA in dye orientation, we investigated the dye-containing films prepared with vinyl polymers. Three kinds of polymers were employed for the preparation of films under a magnetic field, which were poly(acrylic acid), poly(vinyl alcohol), and poly(vinyl pyrrolidone) as anionic, nonionic, and cationic water-soluble polymers, respectively. The  $f_0$  values at the absorption bands of the dyes in the obtained polymer films were evaluated to be  $-0.006 \pm 0.005$ ,  $-0.003 \pm 0.003$ , and  $-0.002 \pm 0.003$ , respectively. Thus, there was no angular dependence of the absorbance for polarization light, as judged from their errors. Also, by the polarization microscopic observation, no polymer chain orientation was found for these dye–polymer films. These results suggest that the dyes cannot be oriented in the films without DNA, though the dye molecules themselves should be affected by a magnetic field because of the interaction for their aromatic groups. In other words, the fabrication of dye-oriented films necessarily requires DNA molecules as a template for dye orientation.

**Dependence on the Dye Contents.** To clarify the influence of dye contents on dye orientation, we prepared AcrO–DNA films under a magnetic field from the solutions containing 1, 2, 4, 9, 18, and 35% of the dye with respect to the constant amount of DNA base pairs. The observed  $f_0$  values for linear dichroism are plotted in Figure 6a. The  $f_0$  values were high and almost identical at dye contents less than 4%; however, the values decreased steeply at higher dye contents. The total amount of oriented dye molecules in DNA films is shown in Figure 6b. The amount of oriented dyes increased linearly in the 0–4% range of AcrO contents, where most of the dye molecules seem to be bound with DNA. In contrast, the amount of oriented AcrO decreased at dye contents above 9%. Then, at about 30%, there was almost no orientation observed. This can be interpreted to mean that the excess amounts of dyes inhibit the alignment of DNA chains. The intercalator has more  $\pi$ -electrons in aromatic rings than those of DNA base pairs, so that it may preferably enhance the orientation of DNA chains due to high anisotropic magnetic susceptibility rather than DNA base pairs. However, the addition of a large amount of intercalators would cause the loss of smoothness of DNA chains due to the increase in the content of external-binding forms,<sup>16</sup> so that the liquid crystallinity of DNA in a solution may become weakened. This phenomenon is in agreement with the dye-dependent change in the viscosity of DNA solution, which shows the maximum of viscosity at a certain concentration of dyes such as EtdB.<sup>20</sup> Consequently, in the case of high contents of intercalators, the alignment of DNA chains in parallel becomes difficult.

The equimolar point of monomer and dimer of AcrO is extremely shifted from 0.04 mM for the system without DNA to 4 mM in the presence of 50 mM<sub>bp</sub> DNA. This is well elucidated by Stone et al. in terms of a stacking coefficient.<sup>21</sup> Since the monomer–dimer equilibrium depends on not only the concentration of dye but also that of DNA, the drying process should affect the composition ratio of the dimer and the monomer. It was found that the relative content of dimeric AcrO versus the monomer in the dye–DNA film was larger than that in the solution before drying.

The  $f_0$  values for both the monomer and dimer bands of AcrO were almost identical in each dye–DNA film, as shown in

Figure 6a. This clearly indicates that even the stacked dimer species of dye orientate parallel to DNA base pairs. Since the peak wavelength of the AcrO dimer in DNA–composite film is the same as that in DNA solution, as described above, the dimer should be bound to DNA. However, the binding form of the dimer would not be a monomeric intercalator because the length of the phosphate backbone between the neighboring bases is too short to accommodate the stacked dimer. Probably, the dimers would be in external-binding forms, as reported by Fredericq et al.,<sup>16</sup> even in our film system. Taking into account the dye–DNA ratios examined on the basis of their results, the orientation of the dimers in external-binding forms would be ascribed to the semi-intercalation of a companion molecule of dimeric AcrO.

Similarly, in DAPI–DNA films, the extent of the dye orientation decreased as the dye contents went above about 3% (Figure 6c). The minor-groove binding of the dyes is known to be highly stable in a solution.<sup>11</sup> This is one of the reasons that such dyes are utilized as reagents for the detection and screening of DNA. Actually, the red shift of the UV–vis absorption peak for our DAPI–DNA solid films suggests the stable contact of the dye molecule with DNA. Though the orientations of dyes and DNA chains are sufficiently high in the region of lower dye contents, the excess amount of dyes seems to interfere with the alignment of DNA chains. This would be similar to the case for DNA with a high content of AcrO as mentioned above. Probably, the DNA binding of DAPI as an intercalator at its high concentration may cause the irregularity of the structure of DNA chains.<sup>19</sup> DAPI is reported to be an AT-specific groove-binding reagent, which requires four consecutive AT base pairs.<sup>19</sup> Therefore, the fraction of the DAPI-binding site is estimated to be rather small. This may lead to the low capacity for DAPI in chain-oriented DNA films in comparison with the AcrO–DNA system.

In summary, irrespective of the binding types for DNA, the excess contents of dyes disrupt the orientation of DNA chains in dye–DNA films. In contrast, in the range of less than a critical content of dyes, DNA–composite films with highly oriented dyes can be obtained.

**Fluorescence Anisotropy of Dye–DNA Films.** The fluorescence measurements taken during the excitation with polarized light were carried out with the sample film at rotational angles changed in 30° increments (Figure 7). The commercial dyes, that is, AcrO, EtdB, DAPI, and Hoech, gave the rotational angle dependences with 180° periodicity, which are relatively similar to the respective patterns obtained by UV–vis absorption. Recognizing these periodic patterns also enables us to estimate the DNA-binding manners of the dyes. The phase of the curves for EtdB and AcrO is different from that for DAPI and Hoech by 90°. Obviously, the phase of the curves for the EtdB and AcrO can be ascribed to the intercalation.

Differing from the curves of absorbance showing the rotational angle dependence expressed with the function of  $\sin^2 \phi$ , as shown in Figure 5a–f, the corresponding curves of the fluorescence measurements exhibited somewhat deformed patterns. For example, the shape of the peak for EtdB–DNA film is obviously different from that of the trough in width (Figure 7a). The extent of the difference in the shapes of the peak and trough is small for Hoech and DAPI, which are minor-groove-binding reagents (Figure 7c and d). Theoretically, these characteristic curves can be recognized to be derived from the fourth-order trigonometric functions. By means of a model calculation for various combinations of the angles  $\beta$  and  $\delta$ , which were defined in the Materials and Methods section, we obtained the

different shapes of theoretical curves. Among them, we could choose the probable sets of parameters to fit to the observed plots, though they are not unique solutions for the respective cases due to the complicated and redundant feature of the functions, as expressed in eqs 14 and 15 (see the Supporting Information). The possible values of  $\beta$  and  $\delta$  were respectively obtained as 90 and 90° for EtdB and AcrO, 45 and 170° for Hoech, and 45 and 5° for DAPI. Thus, the intercalators and the minor-groove-binding dyes are distinguishable by fluorescence measurement. The rotational angle dependence of fluorescence anisotropy for RhoB (Figure 7e) was attributed to the type of intercalator, but the amplitude was very small. On the other hand, the RhoB–DNA film prepared by the draw-and-dry method<sup>2</sup> by way of comparison resulted in no orientation of RhoB molecules, so that the weak angular dependence of the magnetically prepared film could be attributed to the direct magnetic effect on RhoB.

The fluorescence anisotropy essentially depends on the motility of the fluorescent dye molecules. In particular, the excited state of the fluorescent molecules seems to undergo some relaxation process even during the form intercalating in DNA. However, we have little information on the behavior of fluorescent molecules. In the case of minor-groove-binding dyes, the motility would be more complicated. These problems may be the cause of the complexity of other models in comparison with our simple model, which has a defined angle of the transition-dipole moment for emission. Nevertheless, the fluorescence anisotropy measurement for dye-bound DNA has an advantage in determining the DNA-binding manner of the dyes, because it is free from a simple magic-angle problem that occurs at 54.7° of the angle  $\beta$ .

**Judgment of the DNA-Binding Mode of Novel Synthetic Dyes by the Composite-Film Method.** We applied the method for preparing dye-oriented DNA films with a magnetic field to the novel synthetic dyes developed for pharmaceutical use, as shown in Figure 8. These compounds have a common heterocyclic moiety made up of five- and six-membered aromatic rings. The angular dependence of the absorbance for linear polarization light was analyzed for the dye–DNA films containing these original dyes (Figure 9). The seven types of dyes, that is, KN5A–KN5E, KN5H, and KN5I, gave curves of the double-valley type, so these dyes can be judged to be the intercalators.

On the other hand, the compounds KN5F and KN5G had curves with little angular dependence, suggesting that these dye molecules are neither usual intercalators nor typical minor-groove-binding dyes. Considering their chemical structures, these two are the only three-ring systems among nine compounds examined here, which may explain some of our results. Interestingly, KN5G showed a peak shift in the UV–vis spectrum, as did most of the KN-coded compounds, so this molecule is likely to interact with DNA.

To obtain detailed information about DNA binding, we analyzed the DNA–composite films of these dyes by fluorescence measurement with a polarization system (Figure 10). The dyes, except for KN5F and KN5G, showed similar patterns in angular dependence on fluorescence anisotropy, which can be superimposed by the curve calculated with the angles  $\beta$  and  $\delta$  both being 90° (figure not shown). These results are indicative of the intercalation for DNA chains and are in agreement with those by UV–vis measurement. It should be noted that the dye KN5G (Figure 10c) resulted in a curve shape similar to those of intercalators (Figure 7a and b). However, KN5G did not show the angular dependence in the absorbance, as mentioned above.



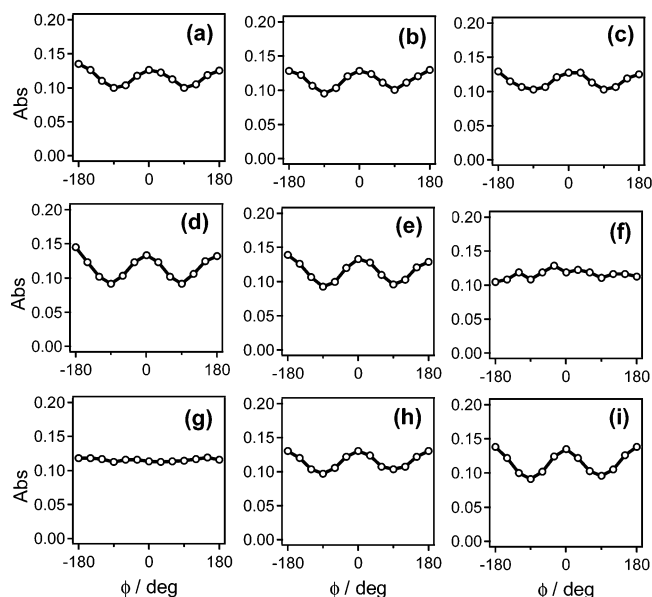


**Figure 9.** Angular dependence curves of the absorbance of DNA-composite films containing nine synthetic dyes, as shown in Figure 8. The absorbance was measured by the linear polarization UV-vis spectroscopy. The contents of dyes were 4 mol %. The respective graphs are shown in a similar arrangement to the corresponding formulas in Figure 8. The synthetic dyes are KN5A (a), KN5B (b), KN5C (c), KN5D (d), KN5E (e), KN5F (f), KN5G (g), KN5H (h), and KN5I (i).

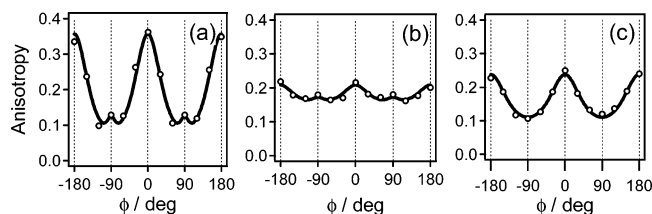


**Figure 10.** Dependence of fluorescence anisotropy on the rotational angle of the dye-DNA films. The data were collected for the films containing 3 mol % dye: KN5A (a); KN5F (b); KN5G (c). The observed and theoretical fluorescence anisotropy were indicated with open circles and a solid curve. The curve shape of KN5A-DNA film depends on the film thickness to a small extent. For example, in the case of KN5A-DNA film with different thicknesses, it showed a similar pattern to that of Figure 7a.

This means that the transition-dipole moment of absorption would lie at the magic angle ( $54.7^\circ$ ), which leads the value of the orientation function,  $3 \cos^2 \beta - 1$ , to null. Therefore, the probable angles of  $\beta$  and  $\delta$  for KN5G were estimated to be  $54.7$  and  $92^\circ$ , respectively. Taking into account the molecular structure and the peak shift in UV-vis spectrum, KN5G seems to be intercalated between DNA base pairs with a tilted angle.

In contrast, KN5F (Figure 10b) gave a relatively flat pattern but with only small angular dependence, of which the favorable angles of  $\beta$  and  $\delta$  appear to be  $54.7$  and  $110^\circ$ , respectively. Since the core structures of both the KN5F and the KN5G molecules are common three-ring systems, the characteristic behavior of KN5F may be attributed to the long side chain with its potential hydrogen-bonding ability. Probably, most KN5F molecules would bind weakly with DNA in a nonspecific manner, although only a small portion seems to bind in a manner similar to that of KN5G. This special binding mode of intercalation with the angle tilted from the plane of the base pairs, which might be called "tilted intercalation", may resemble that of norfloxacin, which has an angle  $\beta$  of  $75^\circ$ .<sup>22</sup>

The data on the fluorescence anisotropy measurement are composed of five independent components corresponding to the

arrangements of the linear polarizations of the first and the second transitions.<sup>14</sup> This is the reason that the rotational angle dependence of the fluorescence anisotropy gave very complicated patterns for respective samples. Unlike with linear dichroism measurement by UV-vis, fluorescence anisotropy measurement for film samples needs to be coupled with the technique to detect the rotational angle dependence including the data at moderately tilted angles. By means of both UV-vis absorption and fluorescence spectroscopies, we were able to successfully judge the DNA-binding modes of novel synthetic dyes. We found the polarization measurement of fluorescence to be especially sensitive to the orientation of the dyes, as discussed above. The additional interesting results were obtained for KN5A-DNA films of different thicknesses. The  $3\text{-}\mu\text{m}$ -thick film gave a peculiar curve with four troughs (Figure 10a), which was different from that for the  $1\text{-}\mu\text{m}$ -thick film, which exhibited a double-valley shape similar to that of AcrO. For these two films of KN5A, the suitable angles of  $\beta$  and  $\delta$  are estimated to be  $80$  and  $100^\circ$  and  $90$  and  $90^\circ$ , respectively. The water content in the film may affect the DNA-binding form of the dye molecules.

In summary, the judgments for our nine compounds by this novel method using dye-DNA films agreed well with those by viscosity for the solutions. These results prove the promise of our dye-DNA-film method. We estimate that one could perform the analysis even with  $0.1\text{ }\mu\text{g}$  of samples by this method at present. This method has superior repeatability and is simple to use. Even if the magnet with dense flux is not available in some laboratories, the alternative methods to orientate the DNA chains may be applicable to this film method.<sup>2,23,24</sup> The only disadvantage of this method may be encountered in the application to dye-DNA systems containing high dye contents, which brings about the disorder of DNA chain alignment, as discussed in previous sections. On the contrary, the problem caused by very low contents of dyes can be solved by superposing the dye-DNA films. Though the direct comparison of our method and a flow dichroism is difficult in a sense because of the difference in the final DNA concentrations of the samples, the practicable easiness of this film method would be a great merit in contrast with the conventional methods such as a flow dichroism.

**Acknowledgment.** This work was supported in part by a research grant from the Foundation for the Promotion of Material Science and Technology of Japan (MST), which is greatly appreciated. The authors are also grateful for a grant-in-aid provided by the Ministry of Economy, Trade and Industry, Japan.

**Supporting Information Available:** Fundamental equations for optical anisotropy. This material is available free of charge via the Internet at <http://pubs.acs.org>.

## References and Notes

- (1) Perkins, T. T.; Smith, D. E.; Larson, R. G.; Chu, S. *Science* **1995**, *268*, 83-87.
- (2) Morii, N.; Kido, G.; Suzuki, H.; Morii, H. *Biopolymers* **2005**, *77*, 163-172.
- (3) Morii, N.; Kido, G.; Suzuki, H.; Nimori, S.; Morii, H. *Biomacromolecules* **2004**, *5*, 2297-2307.
- (4) Veillard, A.; Pullman, B.; Berthier, G. *C. R. Acad. Sci.* **1961**, *252*, 2321-2322.
- (5) Maret, G.; Schickfus, M. V.; Mayer, A.; Dransfeld, K. *Phys. Rev. Lett.* **1975**, *35*, 397-400.
- (6) Brandes, R.; Kearns, D. R. *Biochemistry* **1986**, *25*, 5890-5895.
- (7) Strzelecka, T. E.; Rill, R. L. *J. Am. Chem. Soc.* **1987**, *109*, 4513-4518.



- (8) Yang, C. Y.; Yang, W. J.; Moses, D.; Morse, D.; Heeger, A. J. *Synth. Met.* **2003**, *137*, 1459–1460.
- (9) Kawabe, Y. *Appl. Phys. Lett.* **2002**, *81*, 1372–1374.
- (10) Liang, X.; Asanuma, H.; Komiyama, M. *J. Am. Chem. Soc.* **2002**, *124*, 1877–1883.
- (11) Kristen, C. H.; Bruce, A. A. *Acc. Chem. Res.* **2004**, *37*, 845–853.
- (12) Ijio, K.; Shimomura, M.; Tanaka, M.; Nakamura, H.; Hasebe, K. *Thin Solid Films* **1996**, *284*, 780–783.
- (13) Okahata, Y.; Kobayashi, T.; Tanaka, K.; Shimomura, M. *J. Am. Chem. Soc.* **1998**, *120*, 6165–6166.
- (14) Michel, J.; Thulstrup, E. W. *Spectroscopy with Polarized Light*; VCH Publishers, Inc.: New York, 1986.
- (15) Larsen, T. A.; Goodsell, D. S.; Cascio, D.; Grzeskowisk, K.; Dickerson, R. E. *J. Biomol. Struct. Dyn.* **1989**, *7*, 477–491.
- (16) Fredericq, E.; Houssier, C. *Biopolymers* **1972**, *11*, 2281–2308.
- (17) Carlsson, C.; Larsson, A.; Björkman, M.; Jonsson, M.; Albinsson, B. *Biopolymers* **1997**, *41*, 481–494.
- (18) Shu, D.; Chaires, J. B. *Bioorg. Med. Chem.* **1995**, *3*, 723–728.
- (19) Wilson, W. D.; Tanious, F. A.; Barton, H. J.; Strekowski, L.; Boykin, D. W. *J. Am. Chem. Soc.* **1989**, *111*, 5008–5010.
- (20) Wilson, W. D.; Tanious, F. A.; Barton, H. J.; Jones, R. L.; Fox, K.; Wydra, R. L.; Strekowski, L. *Biochemistry* **1990**, *29*, 8452–8461.
- (21) Stone, A. L.; Bradley, D. F. *J. Am. Chem. Soc.* **1961**, *83*, 3627–3634.
- (22) Son, G. S.; Yeo, J. A.; Kim, M. S.; Kim, S. K.; Holmén, A.; Åkerman, B.; Nordén, B. *J. Am. Chem. Soc.* **1998**, *120*, 6451–6457.
- (23) Taillandier, E.; Liquier, J. *Methods Enzymol.* **1992**, *211*, 307–335.
- (24) Kelly, G. R.; Kurucsev, T. *Biopolymers* **1976**, *15*, 1481–1490.